SUPPORTING INFORMATION

Hyperlensing at NIR Frequencies Using a Hemi-spherical Metallic Nanowire Lens in Sea-urchin Geometry

Ankit Bisht,[a,b] Wei He,[b] Xiaotian Wang,[a] Linda Y. L. Wu,[b*] Xiaodong Chen[a*] and Shuzhou Li[a*]

[a]School of Materials Science and Engineering, Nanyang Technological University, Singapore 639798

[b]Singapore Institute of Manufacturing Technology, 71 Nanyang Drive, Singapore 638075

[*] Correspondence should be addressed to lisz@ntu.edu.sg, chenxd@ntu.edu.sg and ylwu@simtech.a-star.edu.sg

CONTENTS

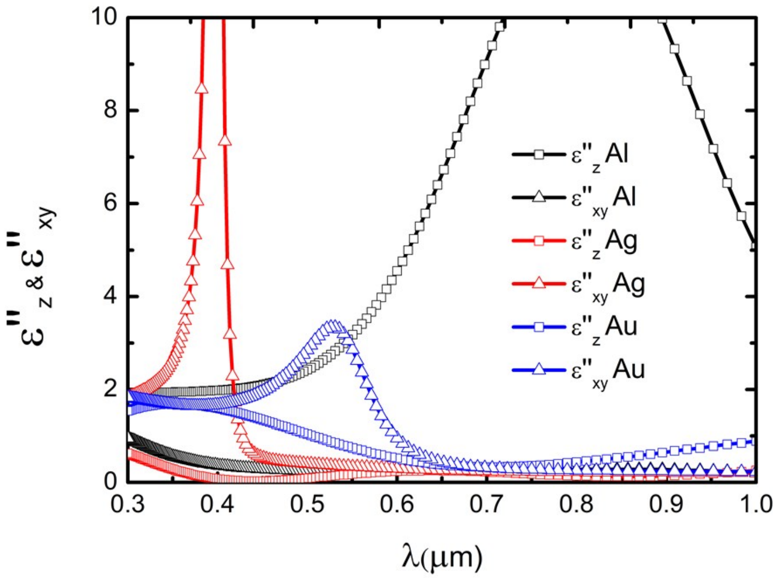

Fig. S1 Imaginary parts of permittivity along z-axis and xy-plane, for Al, Ag and Au

It can be seen from Fig. S1 that in the NIR region both Au and Ag are suitable choices as Al suffers from higher losses. Au suffers higher losses in the visible region, where Ag make up for a better choice. In the UV region of the spectrum, Al constitutes a better material choice as compared to both Ag and Au.

It is to be noted that apart from considering imaginary components of permittivity, the real anisotropic permittivity values have to be considered as well when deciding on the material to be chosen for hyperlensing applications. As can be seen from Fig. 2a, for the chosen nanowire-dielectric system, not only does Al provide negative anisotropic permittivity but also has lower losses in the UV region (Fig. S1). Hence, Al makes for a feasible material choice for hyperlensing in the UV regions of the spectrum.

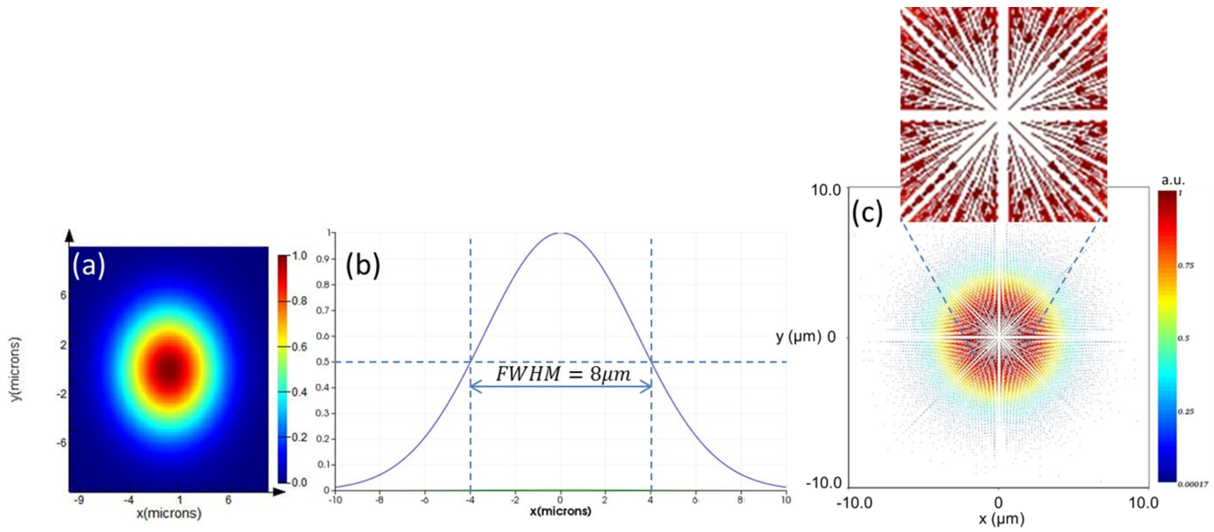

Fig. S2 Field plots of the Gaussian light source injected into the simulation. (a) E-field plot of the radially polarized Gaussian source at a wavelength of 1000 nm. (b) xz plane E-field cross-section at y = 0. The FWHM of the Gaussian source is set as 8 µm. (c) E-field vector profile of the source which is injected into the simulation, with the inset showing the field vectors for radial polarization.

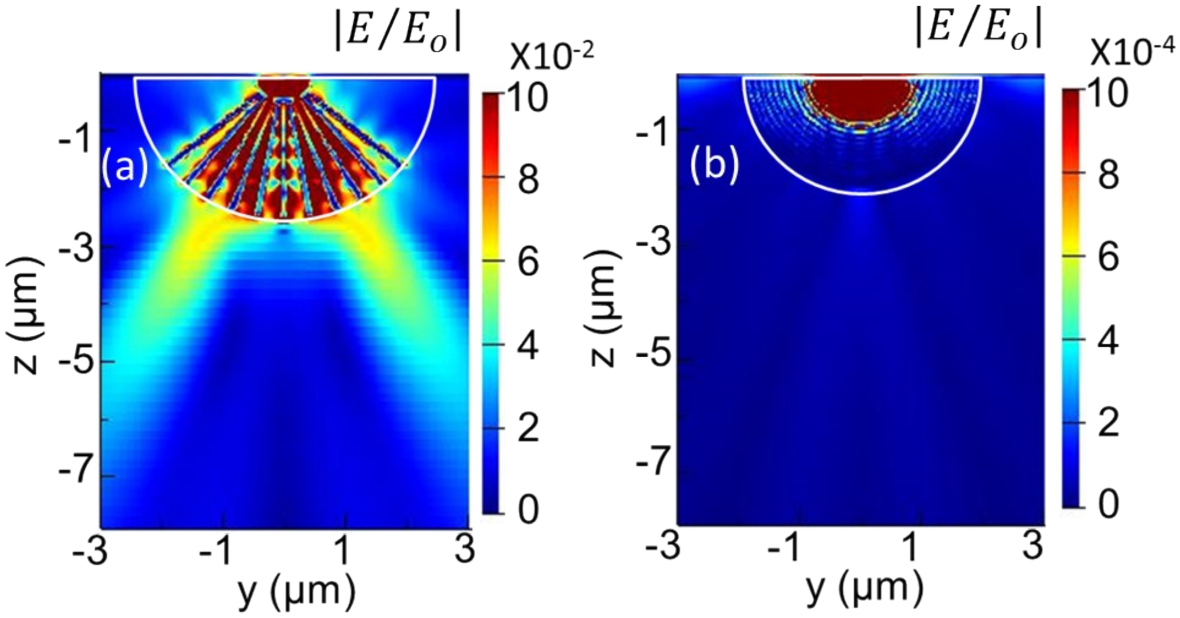

Fig. S3 Normalized E-field plot for light transmission through: (a) SHL (taken from Fig. 5a) and (b) multilayer hyperlens composed of 15 Au/SiO_2 (50 nm/50 nm) layers with a total thickness of ~1.5 μm.

Fig. S3a shows the normalized E-field profile of SHL taken from Fig. 5a while Fig. S3b shows the field profile for a conventional metal-dielectric multilayer hyperlens. The multilayer hyperlens is composed of 15 Au/SiO_2 (50 nm/50 nm) layers, leading to total hyperlens thickness of ~1.5 μm. (It is to be noted that the SHL has a thickness of ~2 μm). All other simulation parameters including light source and field monitors are kept unchanged while transitioning from Fig. S3a to S3b. It can be seen that fields projected by SHL are nearly two orders of magnitude higher than the conventional hyperlens at λ~1000nm. Since multilayer hyperlenses rely on SPR coupling across the metallic layers, under non-resonant conditions most of the energy is dissipated. On the other hand, SHL being non-resonant, allows for higher transmission of incoming energy, as most of the energy is transmitted through the low-loss dielectric regions.

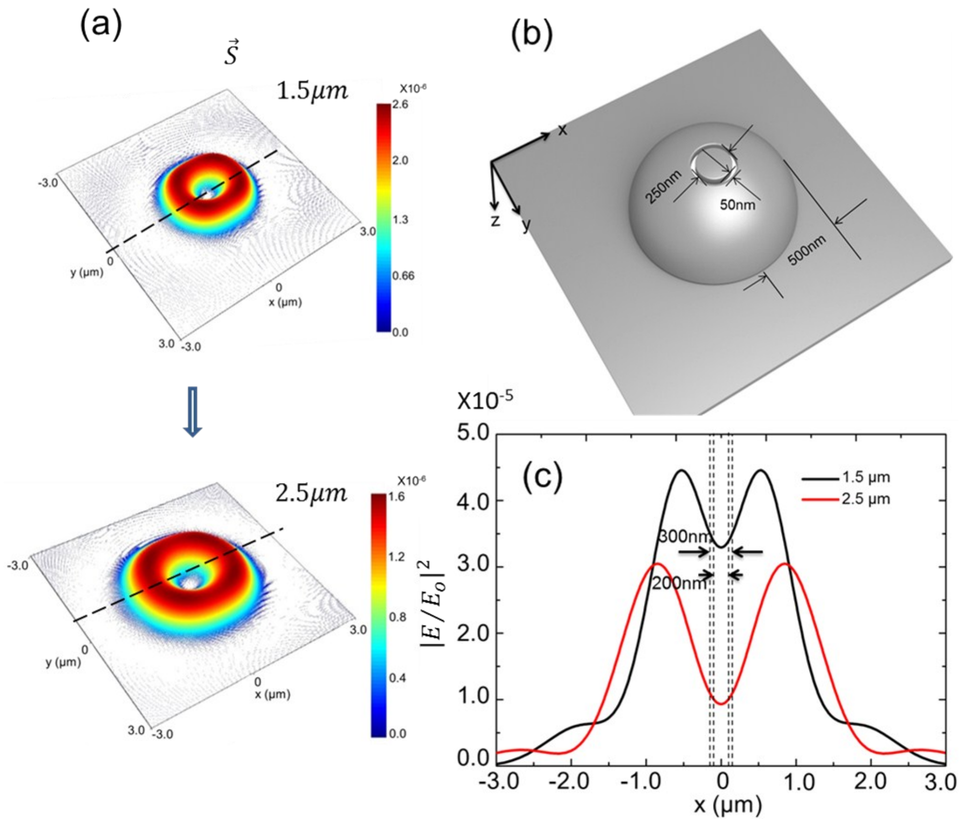

Fig. S4 Smaller nanoring object imaged through SHL. (a) Shows poynting vector plots for the images magnified using SHL structure at different distances below the hyperlens. (b) 3D schematic of the PEC sub-wavelength object, the center-to-center radius is ~250 nm $(\sim\lambda/4)$ while the thickness of the ring is ~50 nm $(\sim\lambda/20)$. (c) E-field intensity plot corresponding to the dashed lines in (a) at different distances below the hyperlens. The dashed vertical lines indicate the size of the nanoring object with outer radius being 300 nm and inner radius being 200 nm.

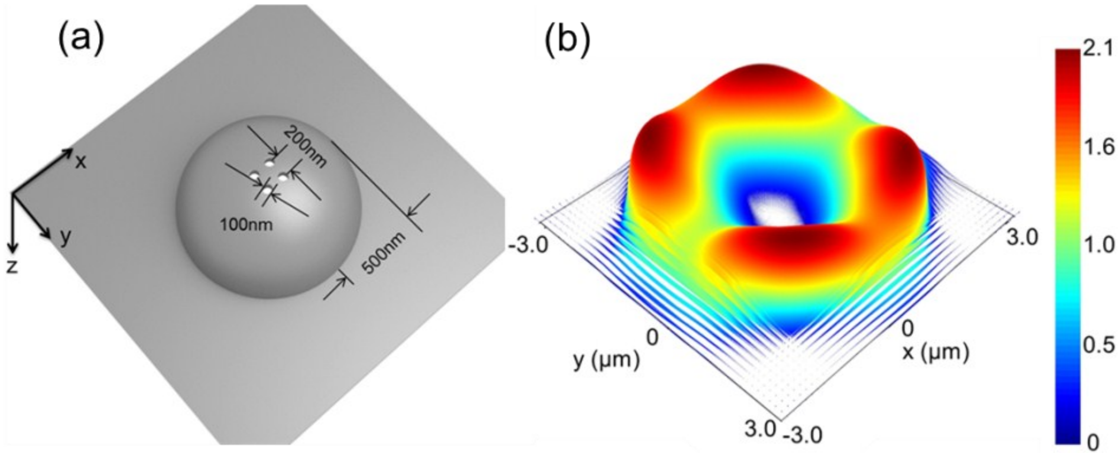

Fig. S5 Quadrumer holed object imaged through the SHL. (a) 3D schematic of the quadrumer holed object, with center-to-center distance between individual holes (along the square edge) being ~200 nm ($\lambda/5$), where the diameter of the individual holes is ~100 nm ($\lambda/10$), (b) corresponding poynting vector plots for the quadrumer object in the far-field, at a distance of 2.5 μm from the hyperlens.

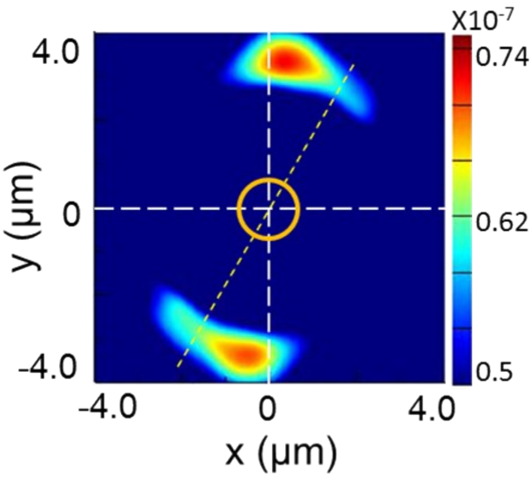

Fig. S6 8 μm by 8 μm poynting vector plot corresponding to Fig. 7c2.

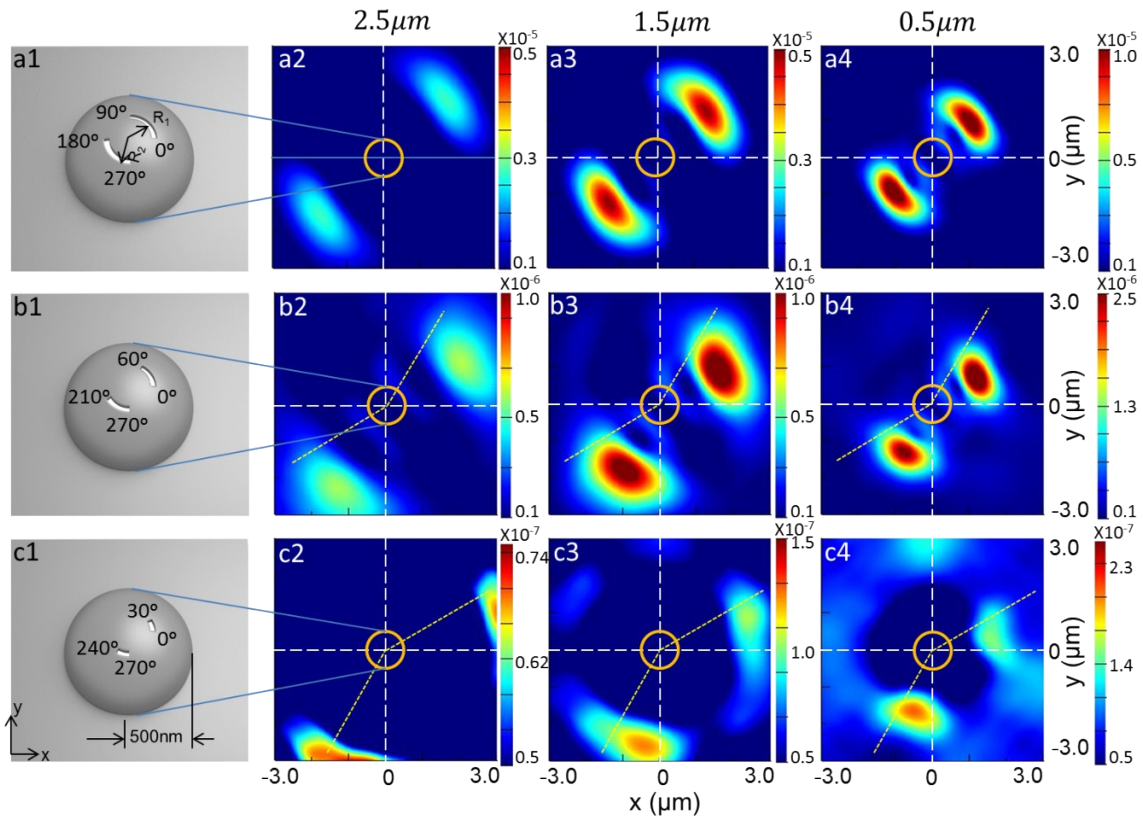

Fig. S7 Poynting vector plots for diffraction limited BNR objects, having single plane of symmetry around the origin. Objects have a decreasing azimuthal span: (a1) 0°-90°, 180°-270°, (b1) 0°-60°, 210°-270°, and (c1) 0°-30°, 240°-270°. The images projected into the far-field, corresponding to their respective objects, are plotted as a function of distance from the bottom surface of the hyperlens, (a4, b4, c4): 0.5 μm, (a3, b3, c3): 1.5 μm, (a2, b2, c2): 2.5 μm.